International Research Journal of Natural and Applied Sciences
Vol. 3, Issue 2, Feb 2016 IF- 2.818 ISSN: (2349-4077)
© Associated Asia Research Foundation (AARF)
Website: www.aarf.asia Email : editor@aarf.asia , editoraarf@gmail.com

FIBER BRAGG GRATING TEMPERATURE SENSOR WITH ENHANCED SENSITIVITY

B.B. Padhy, S.N. Kale, R.B. Sharma and A.D. Shaligram[1]

Defence Institute of Advanced Technology, Girinagar, Pune - 411 025
[1]Dept. of Electronic Science, Savitribai Phule Pune University - 411007

ABSTRACT

Fiber Bragg grating (FBG) temperature sensor has been designed and experimental results have been presented in this paper. Using bimetallic configuration, a temperature sensor with enhanced sensitivity of 71.9 pm/°C and a high-resolution of 0.014°C has been demonstrated. The effect of sensor length (L) on sensitivity has also been investigated.

KEYWORDS: Fiber Bragg Grating, Temperature Sensor, Bimetallic, Enhanced Sensitivity.

1. Introduction

The optical fiber Bragg gratings had made a significant impact in the areas of telecommunication and sensing. The FBG sensors have shown great potential for various applications in the areas of non-destructive evaluation techniques, structural health monitoring and distributed sensing. These sensors are becoming increasingly popular in wide range of industrial, civil and military applications where extreme physical and chemical conditions often make conventional sensors and measurement devices difficult to apply. There are reports on design of FBG and studies on thermal sensitivity of FBG sensors [1-7] for different applications. In general, the bare FBG sensors offer thermal sensitivity of ~ 10-14 pm/°C, which is low in the sense that it may not be sufficient for certain applications where high temperature sensitivity may be desired. Wei Li et. al. have employed a suitable packaging method and have reported thermal sensitivity of 18.64 pm/°C [8].

The present study primarily aims at further enhancing the thermal sensitivity of FBG temperature sensor by using bimetallic configuration. This type of temperature sensor can be effectively used for those applications where there is a need for point or distributed temperature sensing with enhanced sensitivity. The gratings used for temperature sensing

have been inscribed in single mode germano-silicate (glass) fiber using phase mask technique. The Bragg reflection wavelength (λ_B) is centered at 1540 nm.

2. Theory of Fiber Bragg Gratings

FBG is a periodic refractive index perturbation pattern, inscribed in the core of an optical fiber, such that it diffracts the optical signal in the guided mode at specific wavelengths into other core-bounded modes, cladding modes or radiation modes. The spectral characteristics of fiber Bragg grating can be analyzed by Coupled Mode Theory (CMT) [9] derived from the Maxwell equations and applied for the analysis of uniform fiber Bragg gratings.

A fast and accurate technique for investigating the spectral characteristics of fiber Bragg grating is based on the transfer matrix [10] for calculating the input and output fields for a short section of the grating. Each sub-grating is defined by its transfer matrix and the coupled mode equations are used to calculate the output fields of the sub-grating. The output of the first sub-grating is used as the input field for the second sub-grating [11].

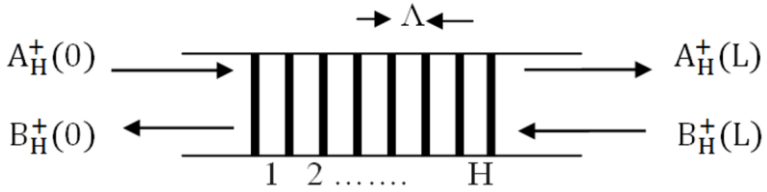

Figure.1. Principle diagram of transfer matrix method for uniform FBG

The mode field amplitudes at z = 0 and z = L can be written as

$$\begin{bmatrix} A_H^+(L) \\ B_H^+(0) \end{bmatrix} = T^H . \begin{bmatrix} A_H^+(0) \\ B_H^+(L) \end{bmatrix}$$

where $A_H^+(0)$ and $B_H^+(0)$ are the forward and backward mode field amplitudes of the grating respectively at $z = 0$, and $A_H^+(L)$ and $B_H^+(L)$ are the forward and backward mode field amplitudes respectively at $z = L$. Fig.1 shows a uniform grating with length L, grating period Λ, individual sub-gratings H (number of grating periods in this case) and total response matrix of the grating T^H. The limit of the grating is defined as $0 \leq z \leq L$ while the boundary conditions of the grating are $[A_H^+(0) = 1]$ at $z = 0$ and $B_H^+(L) = 0$ at $z = L$. This is based on the assumption that the forward going wave is incident from $z = 0$ $[A_H^+(0) = 1]$ and no reflected wave exists $[B_H^+(L) = 0]$ for $z \geq L$, since there is no perturbation beyond the end of the grating. Thus, for the boundary conditions at z = 0, L, we can numerically integrate from z = L to z = 0 to calculate $A_H^+(0)$ and $B_H^+(0)$.

3. Fiber Bragg Grating Sensor

FBG sensors are based on the fact that the Bragg wavelength changes with change in the grating period and/or change in the refractive index. The basic principle of operation of a fiber Bragg grating based sensor system lies in monitoring of the shift in wavelength of the returned Bragg signal, as a function of the measurand (e.g. Strain, Temperature etc.). Thus, any physical parameter which causes changes in the grating period and/or the refractive index can be sensed [12-14] using a FBG by measuring the shift ($\Delta\lambda_B$) in the Bragg wavelength. The Bragg condition is defined as:

$$\lambda_B = 2\,\eta_{eff}\,\Lambda \tag{1}$$

where Λ is the grating period, n_{eff} is the effective refractive index of the core and λ_B is the reflected Bragg wavelength. When strain or temperature is applied to the grating, the effective index of refraction and/or the period of the grating change thereby shifting the Bragg wavelength away from its original value.

To correlate the shift in Bragg wavelength with changes in n_{eff} and Λ in the FBG, one can differentiate equation 1 to get

$$\Delta\lambda_B = 2\,\Delta n_{eff}\,\Lambda + 2\,n_{eff}\,\Delta\Lambda \tag{2}$$

Now dividing equation (2) by equation (1), we get

$$\frac{\Delta\lambda_B}{\lambda_B} = \frac{\Delta n_{eff}}{n_{eff}} + \frac{\Delta\Lambda}{\Lambda} \tag{3}$$

When the bare FBG is subjected to temperature variation, the contribution to the shift in Bragg wavelength ($\Delta\lambda_B$) due to second term on the right-hand side of equation (3) is much smaller than the first term. This is because the fiber elongation ($\Delta\Lambda$) is much smaller as compared to the variation in the refractive index (Δn_{eff}) with temperature.

In view of the above mentioned fact, a FBG sensor was designed by employing a bimetallic configuration so as to obtain larger fiber elongation as compared to bare FBG. This resulted in higher sensitivity of the sensor. The Bragg wavelength shift ($\Delta\lambda_B$) due to temperature can be expressed as [15]:

$$\frac{\Delta\lambda_B}{\lambda_B} = \left[\frac{1}{\Lambda}\frac{\partial\Lambda}{\partial T} + \frac{1}{n_{eff}}\frac{\partial n_{eff}}{\partial T}\right]\Delta T \tag{4}$$

$$\frac{\Delta\lambda_B}{\lambda_B} = (\alpha + \xi)\Delta T \quad (5)$$

where α is the thermal expansion coefficient, ξ is the thermo-optic coefficient of the silica fiber and ΔT is the change in temperature.

4. Sensor Design and Experimental Setup

For the sensor design, two metal strips with different Thermal Expansion Coefficients (TEC) have been attached to the FBG to enhance the temperature sensitivity of the FBG sensor, as shown in Fig 2. The sensor length (L) has been chosen as 60 mm and 100 mm. Lead has been used as the metal with large TEC (Metal-1) and Tungsten as the metal with smaller TEC (Metal-2). The thermal expansion coefficient for Lead is $29.24\times10^{-6}/^{o}C$ and for Tungsten is $4.5\times10^{-6}/^{o}C$. The TEC of Metal-1 is about 6.5 times that of Metal-2. A length of about 180 mm of Metal-2 is attached to the fiber. Then one end of metal-2 is fixed to metal-1. The other end of metal-1 is now fixed to other end of the fiber, as shown in Fig. 2. Alumina paste has been used as adhesive. The curing of the assembly has been carried out at $150^{o}C$ for a duration of two hours to ensure firm adhesion. When the assembly is subjected to temperature variations, the resulting tension is transferred to the FBG sensor due to differential thermal expansion of Metal-1 and Metal-2.

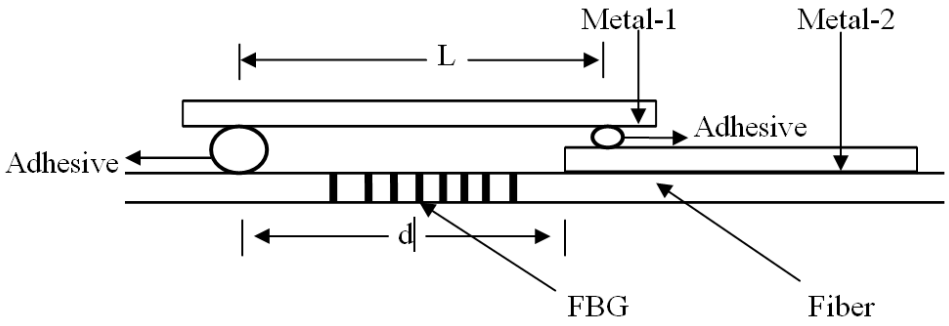

Figure. 2. Bimetallic Sensor Configuration

Here, the elongation has been concentrated only on the FBG when strain due to temperature is applied to the length between the two ends of metal-1 and the fiber attached to metal-2 is sufficiently stiff. If metal-2 is removed from this sensor, the elongation is not concentrated on FBG but is distributed uniformly along the fiber. It is intended to measure the wavelength shifts of reflected FBG spectrum by changing the length of the sensor (lead strip) to investigate the feasibility of this sensor scheme to work with enhanced sensitivity.

When a specific sensitivity is desired, the appropriate length of the sensor can be determined from the experimental data. Higher sensitivity can be obtained by increasing the

length of the metal. Higher sensitivity enhancement may be obtained by using an adhesive to fasten the fiber and metals more tightly. This simple bimetallic configuration has the potential for various applications where high and varying sensitivities are required for multiplexed temperature sensors and other FBG devices.

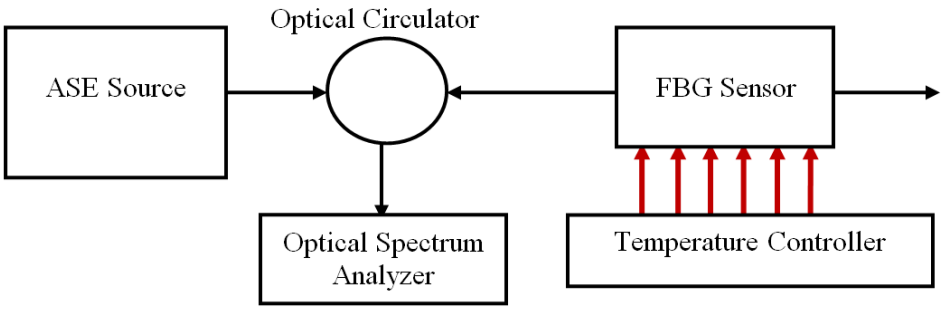

Figure. 3. Experimental Setup

The complete sensor assembly as per the design details shown in Fig.2 is placed inside a temperature-controlled oven. The experimental setup is shown in Fig.3. Light from a C-band Amplified Spontaneous Emission (ASE) broadband source is coupled into the FBG using an Optical Circulator and the shift in the wavelength with change of temperature is recorded with an Optical Spectrum Analyzer (OSA). The FBG is heated from 40°C to 120°C. The corresponding wavelength shift has been observed and the characteristics of the reflected spectrum profile have been analyzed for sensor lengths of 60 mm and 100 mm.

5. Results and Discussion

The experimental studies on enhancement in the thermal sensitivity of the FBG sensor have been carried out along with simulation results obtained by using OptiGrating 4.2 software. In the experiment, the length (L) of the Lead strip has been kept as 60 mm and 100 mm to obtain the desired enhancement in the sensitivity of the sensor.

Fig. 4 shows the sensor response obtained by OptiGrating for the shift in Brag wavelength ($\Delta\lambda_B$) with temperature (T) for bare FBG and sensor lengths of 60 mm and 100 mm. The slope of the ($\Delta\lambda_B$ –T) graph gives the measure of the sensitivity of FBG sensor.

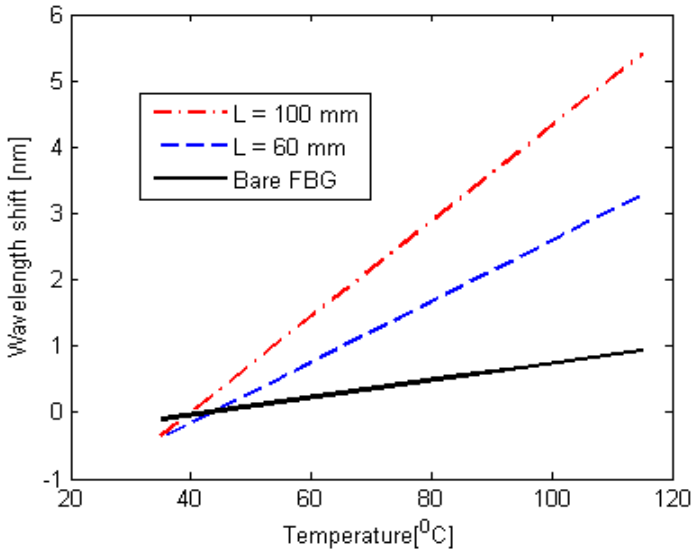

Figure.4. Simulated ($\Delta\lambda_B$ –T) graph for (a) bare FBG (b) L = 60 mm and (c) L = 100 mm

Fig. 4 shows the sensor response obtained by OptiGrating for the shift in Brag wavelength ($\Delta\lambda_B$) with temperature (T) for bare FBG and sensor lengths of 60 mm and 100 mm. The slope of the ($\Delta\lambda_B$ –T) graph gives the measure of the sensitivity of FBG sensor. It can be observed that the slope is higher for sensor length of 100 mm compared to 60 mm. Also, the slope for both of these cases is higher than that of the bare FBG. Thus, enhanced temperature sensitivity can be achieved by increasing the length of the sensor. The $\Delta\lambda_B$ depends on the change in grating period (Λ) and effective refractive index (n_{eff}) of the core. The metal-1 which has higher thermal expansion coefficient causes more elongation (axial strain) in the fiber due to the temperature. This results in higher sensitivity of the FBG sensor.

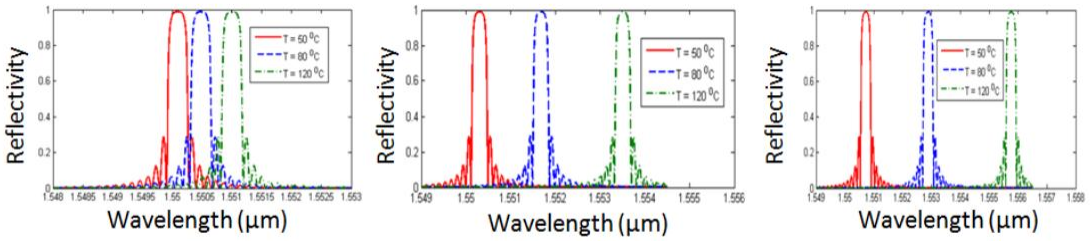

Figure.5. Reflection spectra at 50 °C, 80 °C & 120 °C for (a) Bare FBG (b) L=60 mm (c) L=100 mm

The simulated reflection spectra obtained at temperature of 50, 80 and 120 °C in respect of bare FBG and chosen sensor lengths of 60 mm and 100 mm have been shown in Fig. 5 (a, b & c). It can be inferred from the spectra that at the given temperature, the shift in the wavelength increases linearly with sensor length.

Fig 6 shows the graphs between wavelength shifts with temperature ($\Delta\lambda_B$ –T) for the FBG sensor fabricated in our laboratory. It is observed that the shift in wavelength at a given temperature increases with sensor length. The thermal sensitivities of the FBG sensor are found to be 13 pm/°C, 45.9 pm/°C and 71.9 pm/°C for bare FBG, for sensor length of 60 mm and sensor length of 100 mm respectively. Thus, the enhancement in thermal sensitivity has been achieved. The sensitivity is 3.5 times and 5.5 times that of the bare FBG for the sensor lengths of 60 mm and 100 mm respectively. The results obtained were repeatable for sensitivity calculations. It has also been observed that the sensor has shown linearity and good stability. It is also observed that simulation and experimental results are in good agreement. Keeping in view the fact that the recognized accuracy of FBG signal demodulation is up to 1 pm, the resolution of the enhanced sensitivity sensor is found to be 0.014 °C. Further, for tailoring sensitivity, the relative change in length of FBG is varied by fixing the two metals in such a way that the length of the sensor (L) between the two positions of adhesion varies.

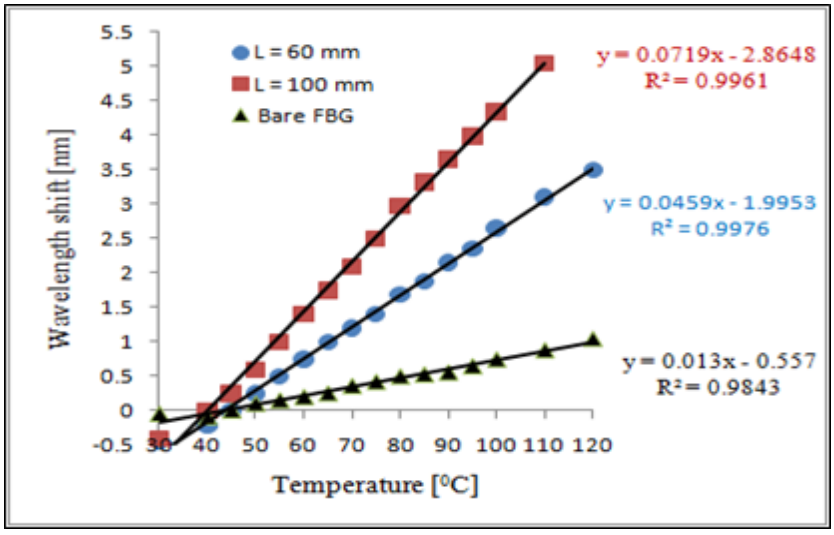

Figure.6. Experimental ($\Delta\lambda_B$ –T) graph for (a) bare FBG (b) L = 60 mm and (c) L = 100 mm

The variation in sensitivity as a function of sensor length is shown in Fig.7. As a thumb rule, if thermal sensitivity desired is more than the conventional sensitivity (~ 14 pm/°C), then bare FBG should be replaced by bimetallic configuration with a sensor length of 20-30

mm. If further higher thermal sensitivity is desired, then sensor length of 60 mm can be used for achieving sensitivity up to 46 pm/°C and sensor length of 100 mm can be used for achieving sensitivity up to 72 pm/°C. We could not investigate more than 100 mm of sensor length due to the non-availability of larger temperature controlled ovens.

In practice, the graph in Fig. 7 can be used as a reference curve for determining the sensor length for achieving a desired sensitivity as per the application. An increase of 1 mm in sensor length is ideal for sensitivity enhancement of 0.57 pm/°C.

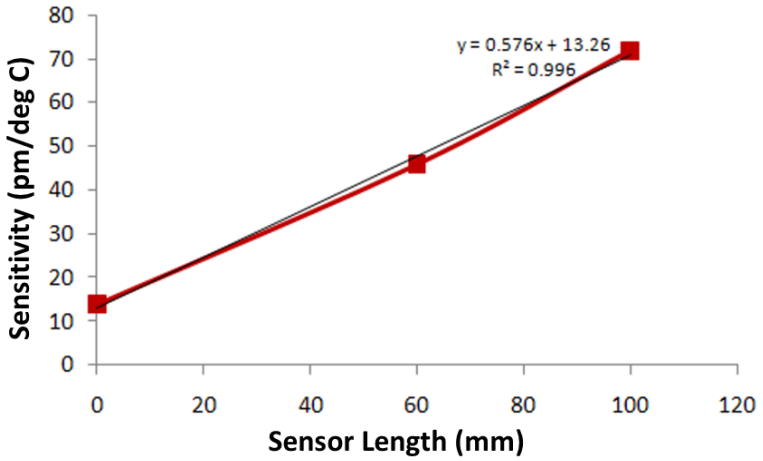

Figure.7. Variation in Sensitivity with Sensor Length

6. Conclusions

The thermal sensitivity of the FBG sensor has been enhanced by attaching two metals with different thermal expansion coefficients and by varying the length of one of the metal strips. Remarkable enhancement of thermal sensitivity up to 7.2 times that of bare FBG has been achieved.

Acknowledgements: The authors would like to thank Defence Institute of Advanced Technology (DU), Girinagar, Pune for providing the research workplace experimental facilities.

REFERENCES

1. K. O. Hill and G. Meltz, Fiber Bragg grating technology fundamental and overview, *Journal of Lightwave Technology, 15*, 1997, 1263-1276.

2. D. Kersey Alan, Michael A. Davis, Heather J. Patrick, Michel LeBlanc, K. P. Koo, C. G. Askins, M. A. Putnam, and E. Joseph Friebele, Fiber grating sensors, *Journal of Lightwave Technology. 15*, 1997, 1442-1463.
3. Y. Tu and Shan-Tung Tu, Fabrication and characterization of a metal-packaged regenerated fiber Bragg grating strain sensor for structural integrity monitoring of high-temperature components, *Smart Mater. Struct. 23*, 2014, 1-11.
4. J. Albert, Li-Yang Shao and C. Caucheteur, Tilted fiber Bragg grating sensors, *Laser & Photonics Rev., 7*, 2013, 83-108.
5. Sunita Ugale and V Mishra, Optimization of Apodized Fiber Bragg Grating for Sensing Applications, *Special issue of Intl. J Comp Applications, 3*, 2011, 8-11.
6. V Rajoria, J Singh, M Tiwari and A Khare, Design and Simulation of Optical Fiber Bragg Grating using Refractive Index and Temperature, *International Journal of Emerging Technology, 2*, 2011, 61-63.
7. A. Othonos and Kalli, Fiber *Bragg Gratings: Fundamentals and Applications in Telecommunications and Sensing* (Artech House, Boston, 1999).
8. Y. Wei Li Weili, Xing-De Han ,Guo-Qing Yu, The Study of Enhancing Temperature Sensitivity for Fiber Bragg Grating Temperature Sensor, in the Proceedings of the Eighth International Conference on Machine Learning and Cybernetics, Baoding, 2009, 2746-2749.
9. B. S. Pun, Y. M. Chang , Chih-Chun Cheng, Yu-Lung Lo and W. Y. Li, An Investigation of Bonding-Layer Characteristics of Substrate-Bonded Fiber Bragg Grating, *Journal of Lightwave Technology*, *23*, 2005, 3907-3915.
10. S.Mathias Müller, Hala J. El-Khozondar, Alessandro Bernardini, and Alexander W. Koch, Transfer Matrix Approach to Four Mode Coupling in Fiber Bragg Gratings, *IEEE Journal of Quantum Electronics, 45*, 2009, 1142-1148.
11. M. Martin, On the Application of Coupled Mode Theory for Modelling Fiber Bragg Gratings, J. Lightwave Technol. 18 (2000) 236-242.
12. Yun Jiang Rao, In-fibre Bragg Grating Sensors, *Measurement Science and Technology, 8*, 1997, 355–375.
13. P. Chojnowski, K. P. Jędrzejewski, Strain and Temperature Sensor Applications of Fiber Bragg Gratings, Photonics Applications in Astronomy, Communications, Industry, and High-Energy Physics Experiments, *Proc. of SPIE Vol. 6347*, 2006.

14. C. C. Yang, M. C. Shih, Gang-Chih Lin, Likarn Wang, and T. J. Chuang, Thermal Performance of Metal-Clad Fiber Bragg Grating Sensors, *IEEE Photonics Technology Letters, 10*, 1998, 406-408.
15. B.D.Gupta, *Fiber Optic Sensors* (New India Publishing Agency, New Delhi, 2006).